ABSORBING BOUNDARY CONDITIONS FOR WAVE PROPAGATION IN VISCOELASTIC MATERIALS

by

Ravi Shankar Badry Badry, Pradeep Kumar Ramancharla

in

17 th World Conference on Earthquake Engineering
(*WCEE*)
: 1
-12

Japan

Report No: IIIT/TR/2020/-1

Centre for Earthquake Engineering
International Institute of Information Technology
Hyderabad - 500 032, INDIA
September 2020

17th World Conference on Earthquake Engineering, 17WCEE
Sendai, Japan - September 13th to 18th 2020

ABSORBING BOUNDARY CONDITIONS FOR WAVE PROPAGATION IN VISCOELASTIC MATERIALS

RS. Badry[1,2], PK. Ramancharla[3]

[1] *Ph.D. Student, International Institute of Information Technology Hyderabad, India, Ravishankar.Badry@research.iiit.ac.in*
[2] *Software Engineer-Engineering software, Arup India Pvt. Ltd, Hyderabad, India, Ravishankar.Badry@arup.com*
[3] *Professor of Civil Engineering and Head of Earthquake Engineering Research Centre, International Institute of Information Technology Hyderabad, India, ramancharla@iiit.ac.in*

Abstract

Radiating boundary conditions are essential in the numerical analysis of infinite domains such as dynamic Soil-Structure-Interaction analysis. Local absorbing boundary conditions proposed by Lysmer and Kuhlemeyer (1969) are widely used in SSI analysis. These boundary conditions are developed based on the wave propagation in elastic materials. However, almost all soil materials exhibit viscoelastic properties. Badry and Ramancharla (2018) proposed the Absorbing Boundary Conditions for wave propagation in viscoelastic materials (VABC). The VABC conditions were developed from the original Absorbing Boundary Conditions (ABC) by including a spring in addition to the dashpot. In fact, these boundary conditions are inefficient when the waves impinge other than normal direction. In this paper, the radiating boundary conditions are modelled using VABC and ALID (Absorbing Layers by Increase in Damping) together to include the advantages of both the boundary conditions and to overcome the drawback of ABC on angle incidence. A detailed numerical analysis is carried out to verify the boundary conditions. The efficiency of the proposed method has been verified for both 1D and 2D wave propagation problems. The efficiency on angle incidence is verified using 2D plane strain model response through spatial Fourier Transformation. The study concludes that the proposed method is simple and reliable method for modelling radiating boundary conditions.

Keywords: Local Absorbing Boundaries, Viscoelastic wave propagation, Rayleigh damping, Soil-Structure interaction, Absorbing Layers by Increase in Damping (ALID)

1. Introduction

Sommerfield radiating boundary condition is one of the major challenges in the finite element analysis of Soil-Structure-Interaction (SSI) problems [1]. Researchers have developed various kinds of formulations over few decades, such as: a). Local Absorbing Boundary Conditions [2-4], b). Absorbing Layers techniques which includes Perfectly Matched Layers [5-11], Caughey Absorbing Layer Method [12-13], Absorbing Layers by Increasing Damping [14-15] and Stiffness Reduction Method [16], c). Boundary element method [17], and d). Infinite elements [18-20].

ABC corresponds to the situation where the boundary is supported on infinitesimal dash-pots oriented normal and tangential to the boundary. Though these boundary conditions are very simple, the major drawback is they are inefficient when the wave impinges the boundary in inclined direction. The key property of a PML that distinguishes it from an ordinary absorbing material is that it is designed such that the propagating waves incident upon the PML from a bulk medium do not reflect on the interface. The ALID consists of defining the absorbing layers at the boundaries of the elastic medium under consideration but requires many absorbing layers which requires much computational time.

The objective of this study is to present a method to combine the absorbing layers (ALID) and local absorbing boundary conditions (VABC) to provide the efficient boundary conditions. This has been achieved by combining the ALID with local Absorbing Boundary Conditions (VABC). The damping characteristics of modified ABC are matched with the absorbing layer near the boundary. Therefore, the reflections due to impedance mismatch between ALID and VABC are avoided. The study also includes the efficiency of the method when the waves impinges other than normal directions

2. Methodology

The equation of motion of the system under dynamic equilibrium is defined as

$$[M]\ddot{u} + [C]\dot{u} + [K]u = F \tag{1}$$

Where $[M]$, $[C]$ and $[K]$ are the global mass, damping and stiffness matrices respectively. $\ddot{u}$, $\dot{u}$, u and F are the acceleration, velocity, displacement and external force vectors respectively. Damping matrix can be defined using Rayleigh damping coefficients as

$$[C] = \alpha[M] + \beta[K] \tag{2}$$

Where α and β are mass and stiffness proportional damping coefficients.

The ALID method uses a material with gradually increasing damping in successive layers such that they absorb incident wave energy and the reflections due to impedance mismatch in successive layers is minimum. At the beginning of the absorbing region, the damping is kept equal to the damping in Area of Study (AoS), zero in most cases and maximum at the end of absorbing region. Thus. the wave entering the absorbing region is gradually damped in the absorbing layers.

Rajagopal et al [15] and Petit et al [16] provided the underlying theory to define the optimal values for absorbing region. This summarises to

- The total thickness of the absorbing layer, L = 1.5 times incident wavelength
- The maximum damping coefficient $\alpha_M = \omega$, where, ω is incident wave frequency
- The damping co coefficient, $\alpha = \alpha_M (x/L)^p$, where, attenuation factor, p = 3 and x is distance from AoS. $x = 0$ at the beginning of the ALID and $x = L$ at the end of ALID.
- The mesh density i.e. minimum number of elements should be 20 per wavelength.
- There is no change in stiffness proportional damping in the absorbing medium

The VABC proposed Badry et al. [4] proposed the Absorbing Boundary Conditions for wave propagation in Viscoelastic medium correspond to a situation where the boundary is supported on infinitesimal dash-pots and springs oriented in normal and tangential to the boundary respectively. The corresponding stress components are given by

$$\sigma = a\ \rho\ V_p\ \dot{u} + 0.5a\ \rho\ V_p\ \alpha\ u \tag{3}$$

$$\tau = b\ \rho\ V_s\ \dot{v} + 0.5b\ \rho\ V_s\ \alpha\ v \tag{4}$$

Where, σ and τ are the normal and shear stresses, $\dot{u}$ and $\dot{v}$ are the normal and tangential velocities respectively; ρ is the mass density; V_s and V_p are the velocities of S-waves and P-waves respectively; a and b are dimensionless parameters. α is mass proportional damping coefficient.

To achieve optimum performance when combining the ALID and VABC, the impedance mismatch between the last absorbing layer and VABC is avoided by replacing α in equation (3) and (4) with the maximum damping coefficient α_M. This indicates that the spring with a coefficient of $0.5\alpha_M\ a\rho AV_p$ is required to add in addition to the standard ABC dashpot with coefficient $a\rho AV_p$ to match the impedance between the ABC and last absorbing layer.

3. Numerical examples

The objective of this section is to demonstrate the efficiency of proposed boundary conditions though various numerical examples and the results are validated. Numerical examples include the 1D, 2D scalar wave propagation problem and 2D elastic wave propagation using the finite element analysis is carried out using explicit integration with lumped mass scheme in a modified version of Oasys GSA [22].

3.1. Wave incidence in normal direction to the boundary

3.1.1 1D p-wave propagation

In this section, efficiency and performance of the proposed boundary conditions are explained for 1D wave propagation models. Two test cases were analysed, first test case to study the performance and second test case is to study the efficiency of the method. In the later test case the efficiency is estimated based on the number of additional degrees of required to model the boundary conditions.

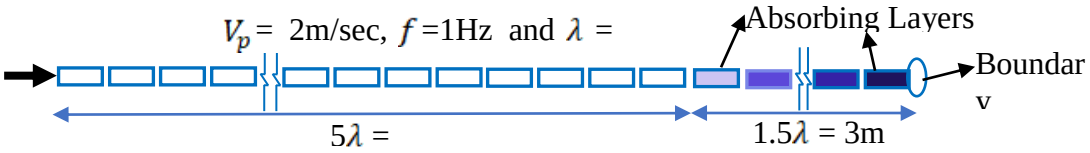

Fig. 1 - Configuration for one dimensional wave propagation model

3.1.1.1 Performance case study:

A 1D model is created to model the elastic wave propagation as shown in Fig. 1. The model is idealised using 2 node bar elements. The material is elastic, Young's modulus and density are taken as 7200 N/m^2 and 1800 kg/m^3 respectively. The primary wave velocity, V_p is estimated as 2 m/sec. The model is assumed to be subjected with predominant wave frequency, f = 1 Hz. The wavelength, λ is estimated as 2m for the incident wave. The length of the model (Area of Study, AoS) is considered as 5λ i.e. 10m. The length of each bar element is taken as 2 mm and the cross-sectional area is taken as 0.1 m^2. The length of element is

arrived such that the change in displacements and stresses in the element are negligible with further reduction in element size.

Three different configurations for radiating boundaries are used, 1. ALID, 2. ALID with ABC and 3. ALID with VABC. Same absorbing layer properties are applied for all the three configurations. Length of the absorbing region is taken as 1.5λ and the element length is same as in AoS i.e. 2 mm. The damping properties are varying along absorbing layers using cubic profile, $\alpha = \alpha_M (x/L)^3$. The damping coefficient, α is taken 0 and α_M at the beginning and end of absorbing region respectively and $\alpha_M = \omega = 2\pi f$. Results from all three models are compared with infinitely extended model, where the model length is such that the reflection from the boundary will not reach the AoS during the analysis.

Load is applied at left end of the member and wave travelling time to reach absorbing layers is 5 sec. The analysis has been carried out for 20 seconds to study the effects of reflection of the wave. Ricker wavelet load is chosen to apply as the predominant frequency

$$U(0,t) = A_f\left[1 - 2\pi^2 f_p^2 (t - t_s)^2\right] e^{-\pi^2 f_p^2 (t-t_s)^2} \quad (5)$$

Where A_f is the amplitude, f_p is the peak frequency and t_s is time shift and the parameters used in this problem are A_f = 1 N, t_s = 4 sec. Peak frequency, f_p is the designed load frequency 1Hz.

The wave propagation forces at the middle of AoS region are shown in the Fig. 2. It is noted from the figure that the reflections due to ALID alone give about 10% and when it combined with ABC and VABC the reflections reduced to 2% and 1.5% respectively. It is also observed that the initial reflections are following the same pattern for all three configurations and then all of them diverge. This indicates that the reflections due to gradual variation of the damping properties in the successive layers in case of ALID+VABC are predominant. ALID with ABC produces more reflections when compared to ALID with VABC as the boundary impedance is not matched with absorbing layers. However, the last two configurations are performing better than ALID alone.

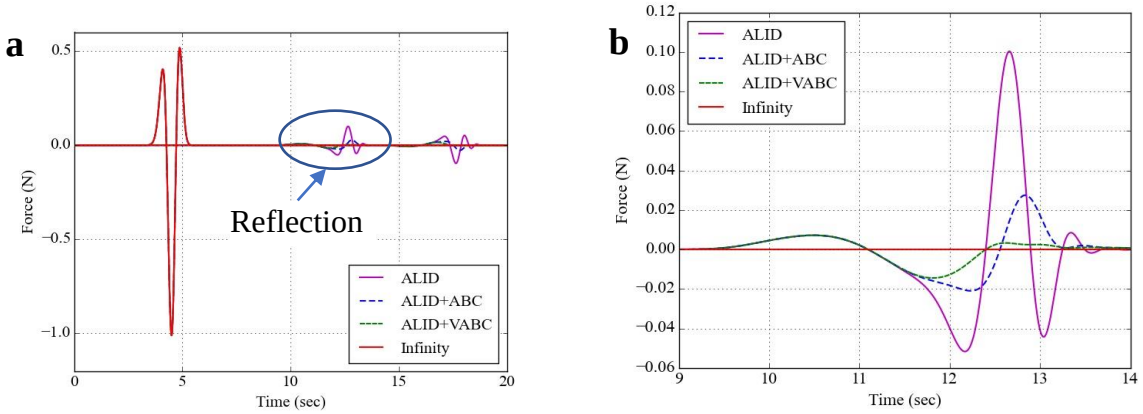

Fig. 2 - Forces in the element at middle of AoS i.e. at 5m for ALID, ALID+ABC, ALID+VABC and Infinity configurations: a) full time record and b) zoomed response for reflections

Fig. 3 shows the displacements due to wave propagation at the middle of AoS region. From the figure, it is studied that the reflections due to ALID alone giving about 15% and when it combined with ABC and VABC the reflections reduced 8% and 5% respectively. It is also observed that the displacements profiles from three configurations follow different trends when compared with infinite medium. The energy absorbed in absorbing layers doesn't allow to resemble the wave propagation when the wave really passes the boundary location. This indicates that the displacements due to wave propagation in the infinite medium

cannot be obtained exactly with absorbing layers, though these layers are efficient in absorbing the wave energy.

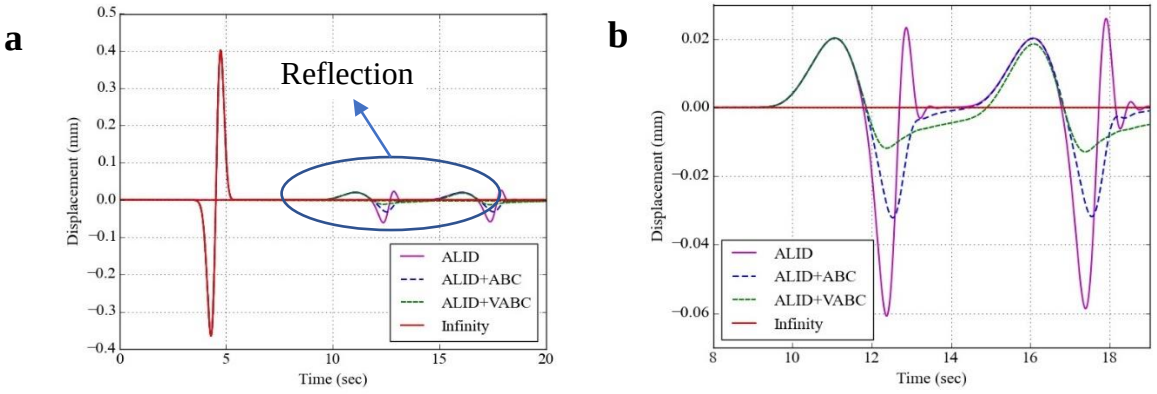

Fig. 3 - Displacement in the element at middle of AoS i.e. at 5m for ALID, ALID+ABC, ALID+VABC and Infinity configurations: a) full time record and b) zoomed response for reflections

3.1.1.2 Efficiency case study:

In this section, the efficiency of the proposed boundary conditions is evaluated by choosing the different absorbing region lengths. The 1D model developed in the previous case study (Fig. 1) is considered along with the same material properties and loading content. The element length is arrived by providing 20 elements per wavelength i.e. 2m/20 = 0.1m. Model is analysed for two different configurations using the absorbing region lengths as λ and 1.5λ, where λ is the wavelength. In the first case 20 elements are provided in absorbing region and in the latter case 30 elements are provided.

Fig. 4 shows the wave propagation forces at the middle of AoS region. From the figure, it is studied that the reflections due to ALID alone yields about 20% and 10% when absorbing region equal to λ and 1.5λ respectively. The reflections in ALID+VABC configuration are reduced to 3% and 1.5% for absorbing region equal to λ and 1.5λ respectively. This shows that even when the length of absorbing region in ALID+VABC configuration is taken as λ, it performs better than ALID with absorbing region length as 1.5λ.

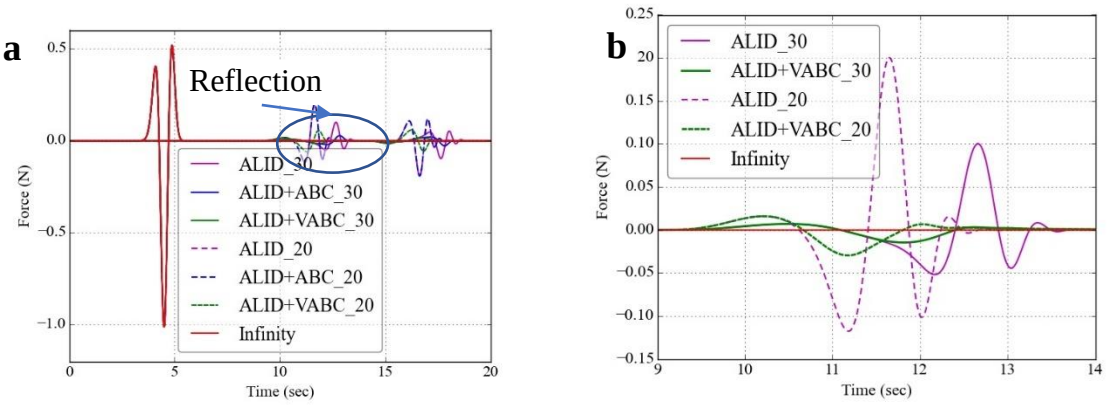

Fig.4 - Forces in the element at middle of AoS i.e. at 5m for 1.5λ and λ : a) full time record, and b) zoomed response for reflections

Fig. 5 shows the displacements due to wave propagation at the middle of AoS region. From the figure, the reflections due to ALID alone giving about 25% and 15% when absorbing region equal to λ and 1.5λ respectively. The reflections are reduced 8% and 5% for absorbing region equal to λ and 1.5λ respectively. It is also noted that the displacements are almost same in both configurations after the wave passes in case of ALID+VABC. This indicates that most of the reflection occurs due to impedance mismatch between the elements.

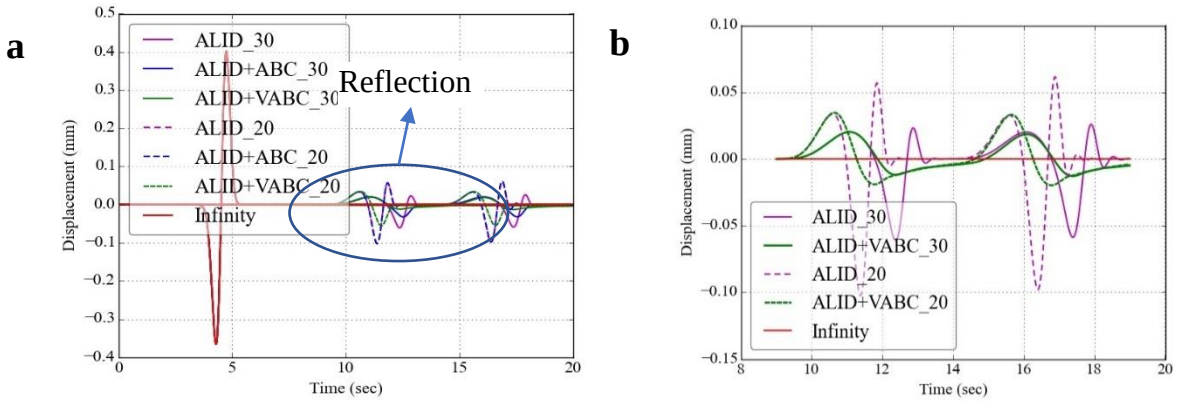

Fig. 5 - Displacements in the element at middle of AoS i.e. at 5m for 1.5λ and λ : a) full time record, and b) zoomed response for reflections

This study concludes that for a design load frequency, the length of the absorbing region can be reduced to λ when using ALID+VABC against to 1.5λ when using ALID. The reduction in absorbing layers in 3D wave propagation impact heavily in terms of total number degrees of freedom.

3.1.2 2D scalar P-wave propagation

In this section, the efficiency of the proposed radiating boundary conditions is evaluated in two-dimensional scalar wave propagation. Pure P-wave propagation resulting from the explosive source in the infinite medium under plane strain condition as described in Fig. 6 is applied.

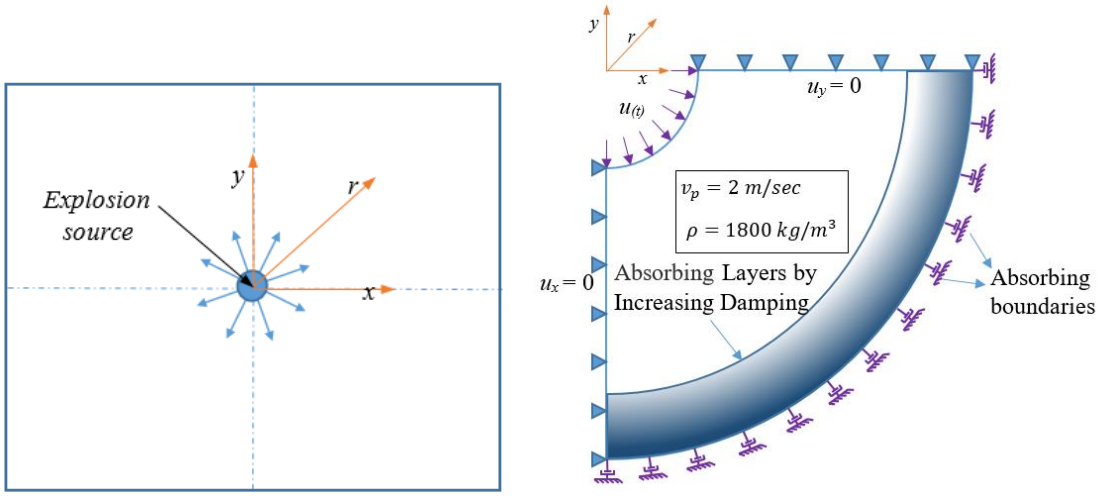

Fig. 6 - 2D Plane strain model for pure P-Wave propagation

The medium has elastic P-wave velocity V_p = 2 m/sec and density ρ = 1800 kg/m^3. The wave travelling time from source field to boundary is approximately 1.5 sec and the simulation duration is 6 sec. Due to symmetry

of the domain, only one fourth of the domain is considered in the modelling and AoS is 4λ i.e. 4.0 m radius. Analysis has been carried out for three configurations as discussed in previous sections. Absorbing region length is considered as 1.5λ and absorbing boundary conditions are applied normal to the boundary as shown in Fig. 6.

The time variation of the displacement at explosion source is considered using a Ricker wavelet as defined in equation (5) with parameters used in this problem are A_f = 10 mm, f_p= 2Hz and t_s = 1.5 sec. A 1.0 m radius cavity is created around the source to apply the pressure wave and to avoid numerical instabilities due to meshing near the origin. To obtain the appropriate source field for use in numerical method, analytical simulation to the infinite media is carried out using

$$u(r,t) = \frac{1}{2\pi}\int_{-\infty}^{\infty}\left\{-i\pi H_0^{(2)}(k*r)F_\omega\right\}e^{+i\omega t}d\omega \qquad (6)$$

Where, r is the radial distance from the source, F_ω is Fourier Transform of Ricker wavelet (5), ω is the frequency, $k = \omega/V_p$ is the wave number. The inverse Fourier transform in equation (6) is performed numerically.

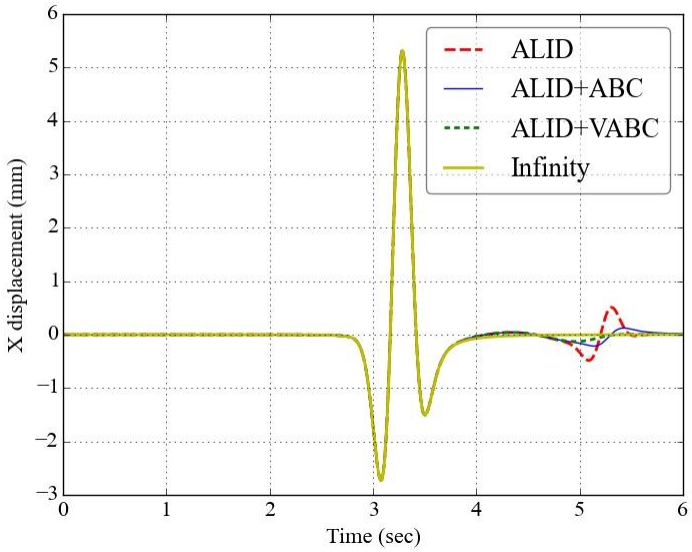

Fig.7 - Displacements at 3.50 m radius

The displacements in the model at 3.5m radius are as shown in Fig. 7. The displacements show a similar pattern to that of one dimensional wave propagation. The reflections in case of ALID configurations is about 10% whereas in case of ABC and VABC with ALID the reflections are about 4% and 3% respectively. However, the percentage of reflections for ABC and VABC with ALID configurations in two dimensional models are about twice as 1D model. Radiation damping effects might be playing a role in reduced efficiency.

Fig. 8 shows the pressure distribution contour plot at 5.5 secs for three configurations. It is noted that the reflections in case of ABC and VABC with ALID are negligible at frequencies higher than designed frequency and the reflections are increased at lower frequencies due to the change in impedance between elements.

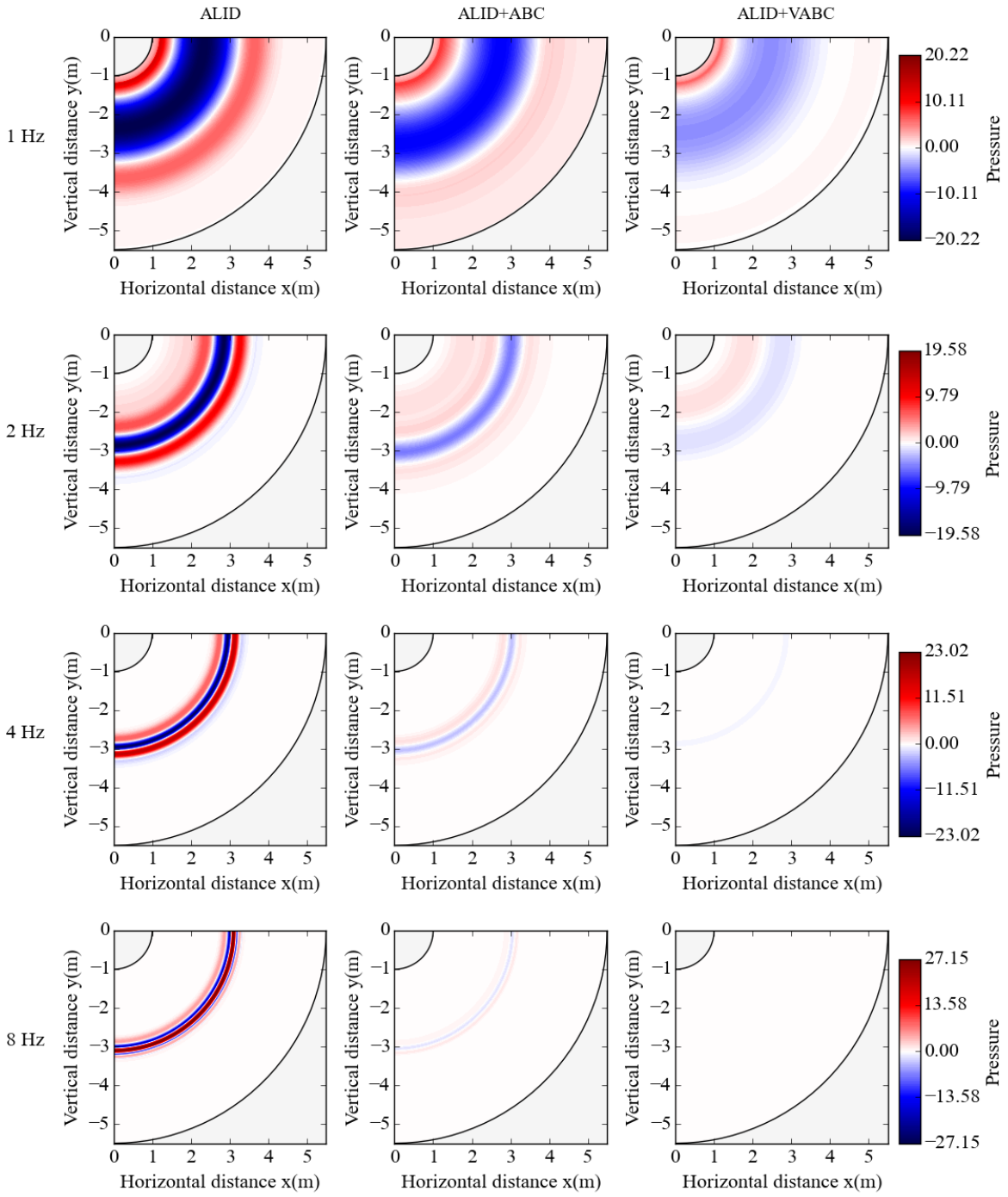

Fig.8 - Snapshot of pressure distribution (N/m2) at time t = 5.5 sec

3.2. Wave incidence other than normal direction to the boundary

A 2D plane strain model is created as illustrated in Fig.9. The material in the medium is elastic with primary and shear wave velocities 2 m/sec and 1 m/s respectively. The ALID absorbing region and VABC are designed for a primary wave with 2Hz loading frequency. The element size is arrived 0.05m in AoS and ALID region. The study boundary conditions i.e. 1). ALID, 2). ALID+ABC, and 3). ALID+VABC are placed at the bottom side and remaining sides are modelled using ultra ALID where the change in absorbing properties are negligibly small.

The model is subjected to hormonic load along the excitation line with a frequency, f = 2. The excitation includes both the primary wave and shear wave with a wavelength of 1.0 m and 0.5 m respectively. Spatial Fourier Transformation is carried out on the displacement response in the AoS region to find the Reflection Coefficients.

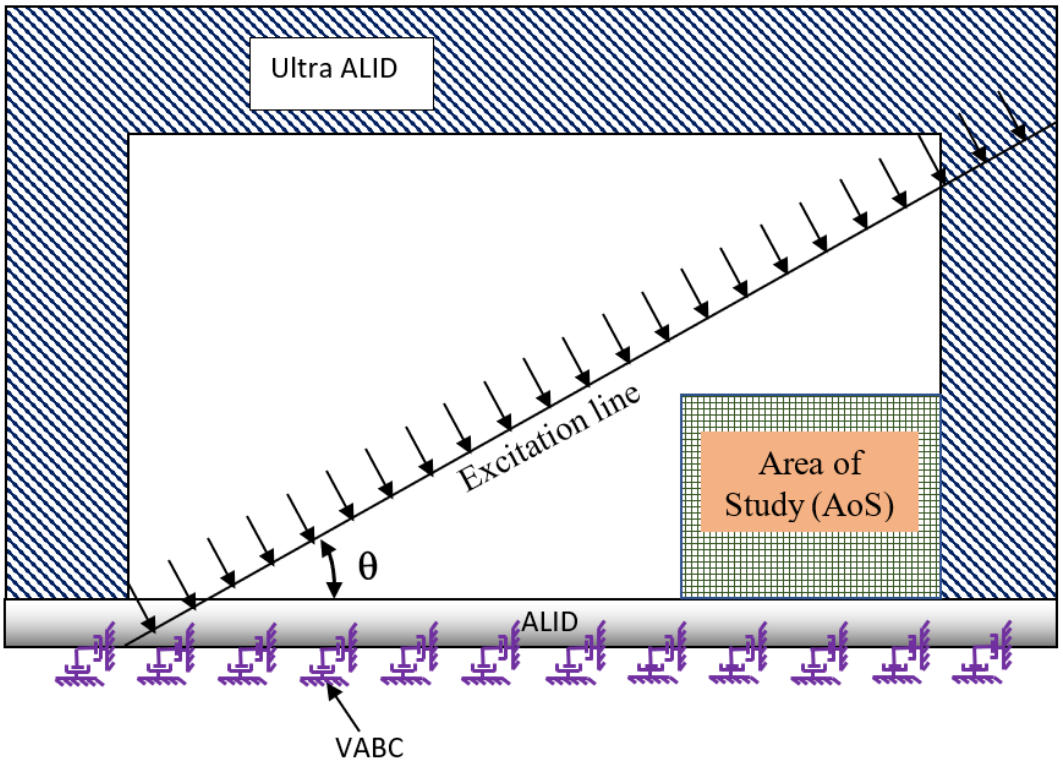

Fig. 9 - 2D Plane strain model for angle incidence

Fig. 10 shows the reflection coefficients for all three configurations. For a P-Wave incidence the efficiency of the all the configuration are increased up to 30 degrees angle of incidence and the efficiencies are decreasing beyond that. The initial increase in efficiency is may due to increase in the absorbing domain length. However, as the incident angle increases the increase in impedance mismatch dominating the effect absorbing length. It is also noted that the difference in efficiency between ALID and other configurations is reducing since the reflections in absorbing region are increasing due to impedance mismatch. Similar observations are also noted for S-Wave incidence as well.

4. Conclusions

In this study, a method for radiating boundary conditions is proposed by combining the absorbing layers and modified absorbing boundary conditions and the following conclusions were drawn:

1. The performance and efficiency of the proposed method is much improved when compared with ALID with minimum additional cost in implementation.
2. The proposed method performs better than ALID alone, even when the length of absorbing region is taken as λ, when compared with the length of absorbing region of 1.5λ in case of ALID. This

reduces the number of elements required by 33% along the length of absorbing region. This reduction in total number of elements will be much more significant when modelling in 3D.

3. The effect of natural frequencies on the performance of ALID or ABC is found to be negligible.
4. The performance degrades when the model is subject to incident wave at a lower frequency than the designed frequency but excellent at higher incident frequencies.
5. The efficiency of the proposed method increases when the angle of incidence increased up to 30 degrees beyond that the efficiency is reducing.
6. The proposed approach uses features that are readily available in many commercial programs, such as Oasys GSA used in this investigation, but the novel feature here is assigning the correct set up and damping properties.
7. It is also noted that, if the loading frequency increases compared to the design load frequency, there is a small degradation in the performance of the proposed boundary condition. However, this is small enough that it would not normally be a concern at such high frequencies.

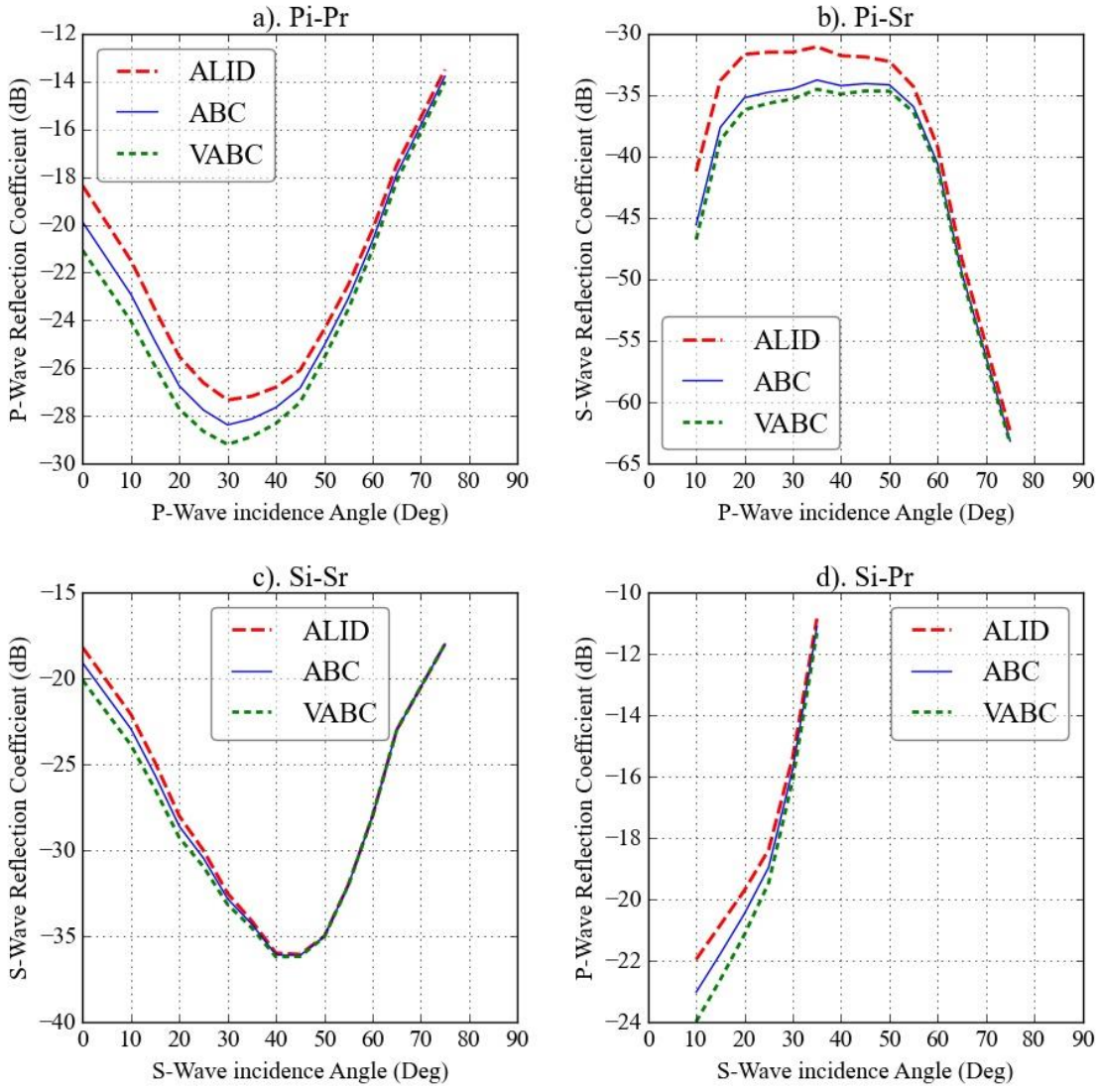

Fig. 10 – Reflection Coefficients

5. Acknowledgment

The authors would like to acknowledge Arup India Pvt. Ltd for financial support to this research.

6. References

[1] Sommerfeld, A., (1949). *Partial Differential Equations in Physics (Vol. 1)*. Academic Press.
[2] Lysmer J., Kuhlemeyer R.L. (1969*). Finite dynamic model for infinite media*. Journal of Engineering Mechanics. Div ASCE 95(EM4):859–877.
[3] Engquist B. and Majda A. *Absorbing boundary conditions for the numerical simulation of waves*, Mathematics of Computation 1977; 31: 629–651,
[4] Badry R.S., Ramancharla P., *Local absorbing boundary conditions to simulate wave propagation in unbounded viscoelastic domains*. Comput Struct (2018); 208:1–16.
[5] Berenger, J.P. *A perfectly matched layer for the absorption of electromagnetic waves*. Journal of Computing in Physics 1994; 114(2):185–200.
[6] Chew W.C., Liu Q.H. *Perfectly matched layers for elastodynamics: a new absorbing boundary condition*, Journal of Computational Acoustics 1996; 4(4): 341-359.
[7] Collino F., Tsogka C. *Application of the PML absorbing layer model to the linear elastodynamic problem in anisotropic heterogeneous media*, Geophysics 2001; 66(1): 294-307.
[8] Marcinkovich C., Olsen K.B. *On the implementation of perfectly matched layers in a three-dimensional fourth-order velocity-stress finite difference scheme*, Journal of Geophysical Research 2003; 108(B5): 2276.
[9] Komatitsch D., Martin R. *An unsplit convolutional Perfectly Matched Layer improved at grazing incidence for the seismic wave equation*. Geophysics 2007; 72(5): 155-167.
[10] Meza-Fajardo K.C., Papageorgiou A.S. *A Nonconvolutional, Split-Field, Perfectly Matched Layer for Wave Propagation in Isotropic and Anisotropic Elastic Media: Stability Analysis,* Bulletin of the Seismological Society of America 2008; 98(4): 1811-1836.
[11] Basu U. Explicit *finite element perfectly matched layer for transient three-dimensional elastic waves*. International Journal for Numerical Methods in Engineering 2009; 77(2):151–176.
[12] Sembalt J.F., Lenti L., Ali G. *A simple multi directional Absorbing Layer method to simulate elastic wave propagation in unbounded domains*, International Journal for Numerical methods in engineering 2010; 1: 1-22.
[13] Andre Rodriguesa A. and Zuzana Dimitrovova Z. *The Caughey absorbing layer method – implementation and validation in Ansys software*, Latin American Journal of Solids and Structures 2015; 12: 540-1564.
[14] Israeli M. and Orszag S.A., Approximation *of radiation boundary conditions*, J. Comp. Phys 1981; vol. 41: 115-135.
[15] P. Rajagopal, M. Drozdz, E.A. Skelton, M.J.S. Lowe, R.V. Craster, *On the use of absorbing layers to simulate the propagation of elastic waves in unbounded isotropic media using commercially available finite element packages*, NDT&E Int. 51 (2012) 30–40.
[16] Pettit J. R., Walker A., Cawley P., and Lowe M. J. S. *A Stiffness Reduction Method for efficient absorption of waves at boundaries for use in commercial Finite Element codes*, Ultrasonics 2014; 54(7): 1868-1879.
[17] Banerjee, P.K., Butterfield, R., (1981). *Boundary element methods in engineering science*. McGraw-Hill Book Co.
[18] Bettess P. *Infinite elements*, International Journal for Numerical Methods in Engineering 1978*;* 11:54-64.
[19] Zienkiewicz O. C., Bando K., Bettess P., Emson C. and Chiam T. C., *Mapped infinite elements for exterior wave problems*. International Journal for Numerical Methods in Engineering, 1985; 21:1229–1251.
[20] Yun C. B., Kim J.M., Yao Z.H., Yuan M.W. *Dynamic Infinite Elements for Soil-Structure Interaction Analysis in a Layered Soil Medium*, Comp. Methods in Engg and Science 2007; 153-167

[21] Chen Xiamoing, Duan Jin, Li Yungui. *Mass proportional damping in nonlinear time-history analysis,* 3rd International Conference on Material, Mechanical and Manufacturing Engineering (IC3ME 2015) 2015; 567-571
[22] Oasys GSA 9.0., Oasys Ltd., London, England, 2018

